Water Research 207 (2021) 117833

Contents lists available at ScienceDirect

Water Research

journal homepage: www.elsevier.com/locate/watres

A fluorescence indicator for source discrimination between microplastic-derived dissolved organic matter and aquatic natural organic matter

Yun Kyung Lee [a], Seongjin Hong [b], Jin Hur [a,*]

[a] Department of Environment and Energy, Sejong University, 209 Neungdong-ro, Gwangjin-gu, Seoul 05006, South Korea
[b] Department of Marine Environmental Science, Chungnam National University, 99 Daehak-ro, Yuseong-gu, Daejeon 34134, South Korea

ARTICLE INFO

Keywords:
Microplastics
Source discrimination
Fluorescence
End-member mixing analysis
Natural organic matter

ABSTRACT

Recently, studies have increasingly focused on the occurrence of plastic leachate and its effects on aquatic environments. However, few studies have aimed to identify microplastic-derived dissolved organic matter (MP-DOM) from environmental samples that are often enriched with natural organic matter (NOM). In this study, three MP-DOM (EPS-DOM, PVC-DOM, and PET-DOM) and eight aquatic NOM samples, and their mixtures, were used to identify a unique optical surrogate for MP-DOM within background NOM. Three major fluorescence peaks (peaks P, H, and L) were identified in the excitation emission matrix (EEM) spectra of both DOM sources (i.e., MP-DOM and NOM). The first two peaks were more pronounced for MP-DOM than for aquatic NOM, whereas peak L showed the opposite trend. The summed intensity ratio of the ranges of the first two peaks relative to peak L, namely, $(H + P)/L$, clearly distinguished between MP-DOM and NOM samples. The MP-DOM source discrimination capability was compared for several selected spectroscopic indices by tracking their changes in the mixtures of two source groups with increasing fraction of MP-DOM via end-member mixing analysis. This was further evaluated based on the three criteria built on the significance of the difference between the two groups, the correlation coefficients of the regressions, and the minimum fraction of MP-DOM in mixtures that can be distinguished from 100% NOM samples. Irrespective of the plastic type and leaching conditions (i.e., UV-irradiated or not), the new optical index, $(H + P)/L$, was superior at distinguishing MP-DOM from the mixtures when compared to other commonly used optical indices. The new index can serve as a sensitive, robust, and reliable fluorescence indicator with minimal interference from NOM for detecting plastic leachate in aquatic samples.

1. Introduction

Increasing amounts of uncontrolled plastic disposal and its subsequent environmental impacts have become a critical global issue. In particular, research has focused on micro-sized plastic particles (i.e., microplastics or MPs) that are unintentionally generated from initial waste materials during their transport to the ocean via rivers or coastal systems (Galloway et al., 2017; Su et al., 2020). In addition to the occurrence of MPs in various environments, dissolved organic substances leached from disposed MPs (referred to as plastic-derived DOM) are another critical aspect for understanding the fate and environmental significance of MPs (Romera-Castillo et al., 2018). The degree of leaching from MPs and the characteristics of plastic-derived DOM are dependent on the weathering processes exerted on MPs, such as exposure to UV light (Potthoff et al., 2017; Zhu et al., 2020). Plastic-derived DOM actively interacts with environmental media and other pollutants (Lee et al., 2021; Lee and Hur, 2020). This phenomenon is more pronounced when MPs are exposed to sunlight or UV light devices installed in treatment facilities, as MP exposure to UV stimulates the release of plastic–derived DOM from MPs (Egessa et al., 2020; Shen et al., 2020).

Given that plastic-derived DOM may contain several additives and/or carbon-chain scission products, and that many of these substances are

Synopsis: The new $(H + P)/L$ ratio can serve as a fast, reliable, and robust fluorescence proxy with minimal interference from NOM to detect plastic leachate in aquatic samples.

* Corresponding author.
E-mail address: jinhur@sejong.ac.kr (J. Hur).

https://doi.org/10.1016/j.watres.2021.117833
Received 4 August 2021; Received in revised form 15 October 2021; Accepted 31 October 2021
Available online 3 November 2021

light-absorbing (Gewert et al., 2018; Suhrhoff and Scholz-Böttcher, 2016), it is necessary to explore the feasibility of detecting these plastic-derived substances by employing UV–visible and/or fluorescence spectroscopy. This idea is partly supported by many previous examples of applying fluorescence spectroscopy to probe the occurrence and dynamics of naturally occurring DOM (Carstea et al., 2016; He et al., 2016; Jaffé et al., 2014). Regarding the optical probing of plastic-derived DOM, a few recent studies (Spagnuolo et al., 2017) have examined protein-like fluorescence features of bisphenol A that were leached from plastics as a common additive. More recently, Lee et al. (2020a) demonstrated that protein-like fluorophores were optical proxies for plastic-derived DOM, which is likely to contain additives and plastic polymers. They further found that a humic-like fluorescence peak was a distinctive signature of plastic-derived DOM produced under UV irradiation. However, these fluorescence signatures from plastic-derived DOM highly overlapped with those of natural organic matter (NOM), which hampered their applicability as a probing index for plastic-derived DOM in aquatic systems enriched with NOM(Lee et al., 2021, 2020a).

Optical indices derived from simple calculations, such as relative abundance or the ratio of different optical features, have been widely used to identify and track DOM sources and also to characterize DOM dynamics due to their advantages of high sensitivity, ease of analysis and online monitoring, and low cost (Derrien et al., 2017; Li and Hur, 2017). The application of these spectroscopic indicators for source discrimination is primarily rooted in the differences in the light-absorbing DOM levels at a particular wavelength across contrasting end-members or different source samples (Derrien et al., 2019; Lee et al., 2018; Yang and Hur, 2014). For instance, Lee et al. (2018) proposed several reasonable criteria for selecting a reliable discrimination index that is least affected by biogeochemical processing among the commonly used indices, such as the biological index (BIX) (Huguet et al., 2009), specific UV absorbance (SUVA) (Weishaar et al., 2003), and the fluorescence index (FI) (McKnight et al., 2001). Although the commonly used optical indices have been successful for NOM source discrimination, it is uncertain whether they are still feasible for plastic-derived DOM because the previously reported proxies were all based on the inherent characteristics of aquatic NOM only. In this context, it is necessary to unearth a reliable optical proxy for identifying plastic-derived DOM in environmental samples containing background NOM. Moreover, the effort to find out the proxy can be further developed into the basis of a cost-effective screening tool for the initial detection of MPs before applying conventional detection methods, such as infrared spectroscopy or particle counting.

To the best of our knowledge, previous studies have not yet suggested a new spectroscopic indicator to probe plastic-derived DOM in NOM-containing environmental samples. In this context, this study specifically aimed to (1) compare the spectroscopic characteristics of DOM leached from two commercial MPs in different NOM background solutions (e.g., rivers, lakes, streams, and wastewater effluents); (2) evaluate the source discrimination capabilities of several selected optical parameters, including newly proposed indices at varying mixing ratios of plastic-derived DOM and aquatic NOM (i.e., two DOM end-members); and (3) provide insight into the applicability of a new spectroscopic proxy for detecting MP contamination in aquatic samples.

2. Materials and methods

2.1. Preparation of microplastic-derived organic matter (MP-DOM)

Expanded polystyrene (EPS), polyvinylchloride (PVC), and polyethylene terephthalate (PET) were selected as the representative plastics in this study. EPS and PET represent buoyant plastic types with a relatively low density, which are more likely to be impacted by sunlight in aquatic environment compared to the non-floating PVC particles. Commercial plastics were purchased in sheet form (1 mm in thickness) for PVC (as windshield) and PET (as part of facial mask), and as beads (1 mm in diameter) for EPS from a local market in Seoul, South Korea. The sheet types of plastic were cut into pieces of approximately 1 × 1 mm, which were then sufficiently washed with distilled water to remove any impurities that might occur during sample handling.

For MP-DOM samples as end-members, leaching experiments were conducted in an artificial freshwater solution containing 5.0 g-plastic/L under two leaching conditions (i.e., under dark and UV irradiation conditions). The leaching solution was composed of $NaHCO_3$ (96 mg/L), $CaSO_4$ (47.4 mg/L), $MgSO_4$ (122.86 mg/L), and KCl (4 mg/L) (Majedi et al., 2014). The UV irradiation was intended to simulate an environment in which the plastic pieces are exposed to sunlight for a long period of time. In this experiment, the leaching lasted for 14 days (Lee and Hur, 2020; Suhrhoff and Scholz-Böttcher, 2016). The MP doses in the solution was set higher than the range typically observed in natural environments (Alimi et al., 2018; Chae and An, 2018) to obtain the maximum amount of MP-DOM for further end-member mixing. For the UV irradiation setting, the freshwater solutions containing the MP pieces were transferred to quartz beakers (1 L) that had previously been autoclaved at 120 °C for 15 min. The leaching was performed in beakers in triplicate. For the leaching experiment with exposure to UV light, a beaker was placed in the center of a closed cabinet with six 8 W UVA lamps (Sankyo Denki, F8T5BL) as the light source. The reactor temperature was maintained at 25 ± 3 °C by circulating cooling air with fans (Phong and Hur, 2015). The top of the beaker was covered with aluminum foil to prevent the volatilization of the solution. A stirrer was placed at the bottom of each beaker for continuous mixing throughout the leaching period. At the end of leaching, the mixing solutions were filtered through pre-ashed Whatman GF/F filters to obtain the MP-DOM samples. A glass vacuum filtration device was used to avoid unnecessary contact with any extraneous plastic material. The final dissolved organic carbon (DOC) concentrations of the MP-DOM samples were 0.63 to 0.68 mg-C/L for the dark condition and 1.14 to 3.99 mg-C/L for the UV irradiation setup. For end-member mixing experiment, only UV-irradiated MP-DOM samples were used, in which EPS-DOM, PVC-DOM, and PET-DOM were arbitrarily denoted as MP1, MP2, and MP3, respectively (Table S1).

For another experiment to mimic the real leaching situation in natural and engineered systems (Section 3.4), the artificial freshwater solution was replaced with pre-filtered lake water from Lake Paldang in South Korea (L2) or treated effluent from an industrial wastewater treatment facility (E2) as background solutions at a fixed DOC concentration of 1 mg-C/L. EPS, a buoyant plastic, was selected as a representative plastic type for this study. The leaching process lasted for a shorter time period (i.e., 7 days) but under the same conditions as the previous experiment (both dark and UV irradiation conditions). For the designated leaching time, the reported residence time (~ 7 days) of Lake Paldang as a background solution was taken into account to determine the leaching period (Kim et al., 2002). The added EPS plastic dose (500 and 1000 pieces-EPS/L) was set at a similar level to those previously reported in MP-polluted aquatic environments, which were 0.01 to 519 MP/L in rivers and 338 to 1473 MP/L in wastewater effluents (Pivokonsky et al., 2018). The details of the research method are presented in Figure S1.

2.2. Preparation of end-member DOM and the mixtures

Eight water samples from different sources and locations (river: R1 and R2; lake/reservoir: L1 and L2; stream: S1 and S2; and treated effluent: E1 and E2) were selected as an aquatic NOM source group in contrast to MP-DOM. Suwanee River fulvic acid (SRFA: R1) and Poly Lake fulvic acid (PLFA L1) purchased from the International Humic Substances Society (IHSS: http://ihss.humicsubstances.org/) were also included in the NOM end-member group (Table S1). Powdered IHSS NOM materials (5 mg) were dissolved in 1 L of deionized water to prepare the NOM solutions. The other aquatic NOM samples were

collected from several sources, including the Han River (R2), Lake Paldang (L2), Toypeong stream (S1), Nakhwaam stream (S2), and municipal (E1) and industrial (E2) wastewater treatment facilities from June 2020 to March 2021. Details of the sampling sites are presented in Table S1. All samples were acidified using sulfuric acid in the field to minimize deterioration before they were transported to the laboratory for filtration through a pre-ashed Whatman GF/F filter. The pH was then adjusted to ~7.0 to recover the field pH condition. The initial DOC concentrations of the samples ranged from 1.0 to 10.8 mg-C/L (Table S1).

UV-irradiated MP-DOM and aquatic NOM were diluted to a constant concentration of 1.0 mg C/L and adjusted to pH 7. The two end-members were mixed with ten different volume ratios of 0:100, 1:99, 3:97, 5:95, 10:90, 20:80, 30:70, 50:50, 75:25, and 100:0, in which a ratio of 0:100 represents 100% aquatic NOM, while a ratio of 100:0 represents pure MP-DOM. The MP1 solution (irradiated EPS-DOM) was mixed with all types of aquatic NOM solutions, whereas MP2 and MP3 (irradiated PVC-DOM and PET-DOM) were mixed with the IHSS NOM solutions or SRFA (R1) and PLFA (L1). Thus, a total twelve different solutions of DOM mixtures (i.e., MP1 + R1, MP1 + R2, MP1 + L1, MP1 + L2, MP1 + S1, MP1 + S2, MP1 + E1, MP1 + E2, MP2 + R1, MP2 + L1, MP3 + R1, and MP3 + L1) were considered for end-member mixing experiment.

2.3. Analytical measurements

2.3.1. Dissolved organic carbon (DOC) and UV–vis spectroscopy

DOC concentrations were measured using a total organic carbon analyzer (Shimadzu L-series, TOC—CHP, Japan). Absorption spectra from 200 to 800 nm were scanned at 1 nm intervals using a UV-visible spectrophotometer (UV-1800, Shimadzu, Japan). The absorption coefficients of chromophoric DOM (CDOM) were measured at 254 nm and 355 nm (a_{254} and a_{355}, $a_\lambda = 2.303 \times A_\lambda$/pathlength, where A_λ is the optical density) (Hu et al., 2002). The absorption ratios at 254 to 436 nm and 300 to 400 nm (E2/E4 and E3/E4), and the spectral slope ($S_{275–295}$), which is the slope of a linear regression for the log-transformed absorption spectrum between 275 and 295 nm, were calculated following the definitions in previous literature (Battin, 1998; Claret et al., 2003; Helms et al., 2008).

2.3.2. Fluorescence EEM measurements and parallel factor analysis (PARAFAC) modeling

Fluorescence excitation emission matrices (EEMs) were obtained using a luminescence spectrometer (F-7000, Hitachi, Japan). The EEMs were scanned at emission wavelengths (Em) of 280–550 nm in 1 nm increments over an excitation wavelength (Ex) range of 220–500 nm, with a stepwise increase of 5 nm. The excitation and emission slits were adjusted to 10 nm. The fluorescence responses to distilled water were subtracted from the measured spectra to obtain the final EEM data of the DOM samples. The fluorescence intensities were normalized to Raman units (R.U.) using the fluorescence intensity of an integrated Raman peak at 350 nm (Em) (Lawaetz and Stedmon, 2009). Three commonly used fluorescence indicators for source discrimination were estimated from the EEM spectra: the fluorescence index (FI) (McKnight et al., 2001), humification index (HIX) (Ohno, 2002), and biological index (BIX) (Huguet et al., 2009). The FI is the ratio of the emission intensity at 450 nm to that at 500 nm with an Ex fixed at 370 nm, which has a value of ~1.9 for microbially-derived DOM and ~1.4 for terrestrially-derived DOM (McKnight et al., 2001). The HIX was utilized to indicate the degree of humification in DOM, which was calculated using the emission intensity area from 435 to 480 nm divided by the sum of two intensity areas from 300 to 345 nm and from 435 to 480 nm at 254 nm (Ex) (Ohno, 2002). BIX is a rough descriptor for probing the presence of autochthonous DOM, which is associated with the presence of freshly produced DOM from planktonic or microbial sources. It was calculated using the intensity ratio at 310 nm/380 nm (Ex/Em) to 310 nm/430 nm (Ex/Em) (Huguet et al., 2009).

Parallel factor analysis (PARAFAC) modeling was performed using MATLAB 7.0 (Mathworks, Natick, MA) with the drEEM Toolbox (Murphy et al., 2013). The number of independent fluorescent DOM (FDOM) components was determined using split-half validation of the EEM results from the end-member mixtures ($n = 275$) and the percentage of the explained variance (98.7%). The maximum fluorescence intensity (F_{max}) of the peak of the identified components was used to represent the relative quantities of the individual FDOM components.

3. Results and discussion

3.1. Comparison of spectroscopic features between MP-DOM and aquatic NOM

3.1.1. UV absorption properties

The UV absorption spectra of aquatic NOM and MP-DOM under different leaching conditions (i.e., dark and UV irradiation) are shown in Fig. S2, and five typical absorption-based parameters (two absorption coefficients, two absorption ratios, and spectral slope) were compared (Table S1). The spectra of PVC-DOM and PET-DOM showed a shoulder between 220 and 260 nm, which was not observed in aquatic NOM samples or EPS-DOM. A similar observation of a shoulder at <280 nm in the absorption spectra was previously reported for photo-aged plastic-derived DOM samples (Shi et al., 2021). After exposure to UV light, both MP types released more CDOM, resulting in a higher UV absorption coefficient as compared to the cases without UV irradiation. For example, PVC-DOM exhibited 0.88 ± 0.05 L m^{-1} mg-C^{-1} for dark-treated samples at 254 nm, and 1.74 ± 0.28 L m^{-1} mg-C^{-1} for UV-irradiated samples. The a_{254} and a_{355} values of aquatic NOM samples were higher than those of MP-DOM per the same DOC concentration (a_{254}: 0.88–2.03 m^{-1} mg-C^{-1} for MP-DOM versus 1.99–8.47 m^{-1} mg-C^{-1} for aquatic NOM) (a_{355}: 0.03–0.98 m^{-1} mg-C^{-1} for MP-DOM versus 0.78–5.07 m^{-1} mg-C^{-1} for aquatic NOM). Moreover, the $S_{275–295}$ values of MP-DOM (0.015–0.045) exhibited the opposite trend, which were generally higher than those of aquatic NOM (0.013–0.018). Our results suggest that the aromatic content and average molecular weight of MP-DOM may be lower than those of typical aquatic NOM (Galgani et al., 2018; Lee et al., 2020b). In contrast, the difference in the two absorption ratios (i.e., E2/E4 and E3/E4) between the two DOM end-members was nearly negligible (Student's test, $p = 0.2015$ and 0.4431, respectively), probably because of the poor signals in the longer wavelength range from 350 to 500 nm (Fig. S1).

3.1.2. Fluorescence properties and EEM-PARAFAC modeling

A prominent peak appeared in the protein/phenol-like fluorescence region of MP-DOM irrespective of the leaching conditions and the plastic types (Figs. 1a, 1b, and S3a–S3d), which was similar to peak B (~225 (~280)/~305 nm) defined by Coble (1996). This peak was also observed in other plastic leachates containing bisphenol A, which is a phenol-like fluorescent substance(Spagnuolo et al., 2017) as well as in wastewater samples comprising lignin, phenols, and polyaromatic hydrocarbons(Huang et al., 2012; Navalon et al., 2011). The dominant peak was assigned to peak P in the present study. The fluorescence intensity of peak P was much more pronounced in MP-DOM samples obtained under UV light than in the dark (0.113 to 0.139 R.U. for dark-treated samples versus 0.173 to 0.197 R.U. for irradiated samples). Furthermore, the DOC-normalized peak P intensities of all MP-DOM samples were more than six-fold higher than those of aquatic NOM (Figs. 1e and 1f). For example, the peak P intensities of MP-DOM ranged from 0.113 to 0.196 R.U., whereas those of aquatic NOM ranged from 0.031 to 0.108 R.U.. The predominance of protein/phenol-like fluorescence features in this study was consistent with previous observations of other MP-DOMs (Lee et al., 2020a; Luo et al., 2019). Regardless of plastic types, a notable difference in the EEMs between the dark- and the UV-treated MP-DOM was the occurrence of additional peaks in the humic-like region at Ex/Em of 230/405 nm and 290/405

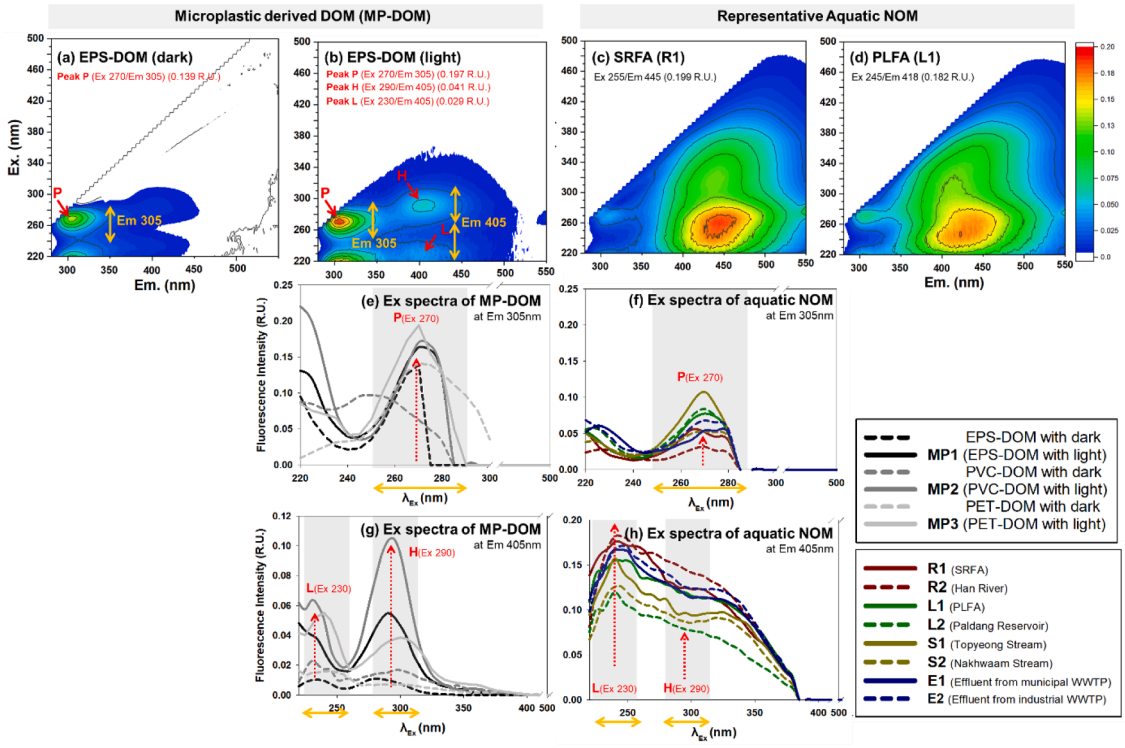

Fig. 1. Fluorescence EEM spectra of the DOM leached from commercial EPS with and without UV irradiation after 14 days of leaching (5 g-MP/L) (a: dark-treated EPS-DOM, b: irradiated EPS-DOM) and two representative aquatic NOM samples (c: SRFA, d: PLFA). The letters and arrows in red indicate the positions of three major peaks (Peaks P, H, and L). Peak P is assigned to a phenol/protein-like fluorescence, while peaks H and L represent humic-like fluorescence features of MP-DOM centered at a longer (Ex/Em: 230/405 nm) and shorter (Ex/Em: 290/405 nm) wavelength, respectively. The DOC concentrations of the prepared solutions were adjusted to 1 mg-C/L. Comparison of the excitation spectra between (e and g) MP-DOM (EPS-DOM and PVC-DOM) and (f and h) aquatic NOM samples (river, lake/reservoir, stream, and effluent water) at a fixed excitation wavelength of 305 and 405 nm, respectively.

nm for the latter (Figs. 1b and S2b), which were also reported in other MP-DOM studies (Lee et al., 2021, 2020a). In this study, the humic-like peaks at 290 nm (Ex) and 230 nm (Ex) were designated as peaks H and L, respectively. Two peaks were also observed in the aquatic NOM samples (Figs. 1c, 1d, and S3e to S3j). However, we observed a clear difference in the peaks between MP-DOM and the aquatic NOM samples. Peak L was more pronounced than peak H in the aquatic NOM samples, while the higher intensity of peak L relative to peak H was not observed for MP-DOM. Meanwhile, peak H exhibited a much higher intensity than peak L for the irradiated MP-DOM samples. The dark-treated MP-DOM samples showed similar levels of the two peak intensities (Figs. 1g and 1h). For example, the intensities of peaks H and L were 0.103 R.U. and 0.064 R.U., respectively, for the UV-irradiated PVC-DOM (Fig. 1e).

These distinctive features between MP-DOM and aquatic NOM can produce a source discrimination index consisting of peaks H, P, and L in a way that maximizes the discrimination between the two DOM end-member groups. The ratio of H/L can distinguish between irradiated MP-DOM and aquatic NOM. Furthermore, the extremely high intensity of peak P in dark-treated MP-DOM can also be effectively used to discriminate MP-DOM from aquatic NOM in the absence of UV light (i.e., no humic-like fluorescence peak). However, the exact location of the peaks might vary slightly depending the type of samples or the conditions of the instrument. For example, the position of the highest peak of un-irradiated PVC-DOM (i.e., Ex/Em of 250/305 nm) did not coincide with that of peak P (i.e., Ex/Em of 270/305 nm) (Fig. S3a). To compensate for this variation, an excitation wavelength region with 40 nm- interval at a fixed emission wavelength was considered to define the peaks P, H, and L, as shown in Figs. 1e-1h. In other words, Ex/Em of 250–290/305 nm, 270–310/305 nm, and 220–260/405 nm were designated as the integrated ranges of peaks P, H, and L, respectively. In previous literature, several fluorescence indicators have been derived from the intensity ratios of different wavelength ranges rather than ratios of individual peaks (Heo et al., 2016; Ohno, 2002). In the present study, we proposed a relative ratio of the integrated regions of the three peak ranges, namely, $(H + P)/L$, as a source discrimination index for MP-DOM. The suggested index, $(H + P)/L$, showed significant differences between MP-DOM and aquatic NOM compared to the simple ratio of H/L (i.e., H/L) (Fig. 2). A significant difference was observed in the $(H + P)/L$ ratios between the two groups irrespective of the leaching conditions (i.e., dark versus UV-irradiation) (Student's *t*-test, $p < 0.001$), while the difference in the simple H/L peak ratio was negligible ($p = 0.165$). Moreover, the fluorescence proxies that have been widely used for NOM source discrimination, such as BIX and FI, exhibited insignificant differences between the two groups ($p = 0.729$ and 0.083, respectively) (Fig. S3). HIX values, which represent the relative degree of humification, were higher in the aquatic NOM group (0.706–0.918) than in the MP-DOM samples (0.078 to 0.337) ($p < 0.001$). This result was consistent with the previous observation of the absorption properties, which indicated relatively higher aromatic contents in aquatic NOM than in MP-DOM.

Three different FDOM components were identified via EEM-PARAFAC modeling, which included two humic-like components (components 1 and 2) and one protein/phenol-like component (component 3) (Fig. S6). Their peak locations were compared with those previously reported in the literature on aquatic NOM and MP-DOM (Table S2). Components 1 (C1) and 2 (C2) exhibited maxima at 260 (330)/452 nm and 240(285)/385 nm (Ex/Em), respectively. Component 3 (C3) exhibited its maximum intensity at 270/307 nm (Ex/Em). The two humic-like components (C1 and C2) were analogous to those typically reported in natural aquatic systems (Kowalczuk et al., 2013; Lee et al., 2018; Li et al., 2016) although the feature of C2 partially overlapped with peaks H and L in the previous EEM spectra of the

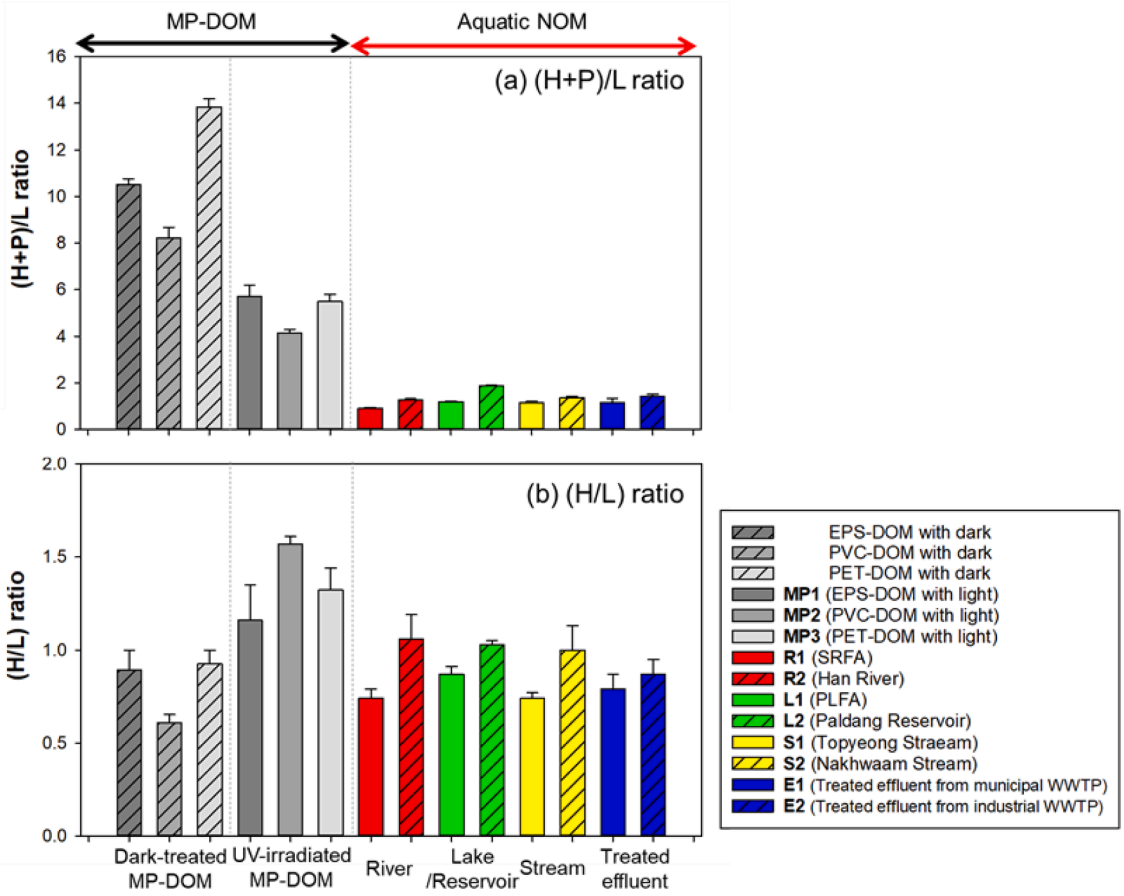

Fig. 2. Comparison of two EEM peak ratios (a: $(H + P)$/L and b: H/L) for different sources of DOM, including MP-DOM and aquatic NOM.

MP-DOM samples. However, the peak location of C3 matched with peak P in the EEMs of the MP-DOM samples. Similar results have been reported for leached solutions from plastic materials(Lee et al., 2020a; Spagnuolo et al., 2017). The MP-DOM group was characterized by the abundant presence of C3 at 74.1%–84.0%, while aquatic NOM was dominated by the other two components (i.e., C1 + C2) at 65.2%–60.2% (Table S2). The relatively higher distribution of the protein/phenol-like component (C3) in the MP-DOM versus aquatic NOM groups was in line with a previous report demonstrating the higher bio-labile properties of MP-DOM compared with aquatic NOM (Romera-Castillo et al., 2018). In this regard, C3 can be considered an indicator of the presence of MP-DOM, whereas C1 appears to be highly linked to aquatic NOM in typical aquatic systems. Although C2 was more abundant in aquatic NOM than in MP-DOM (23.1%–50.1% for aquatic NOM vs. 11.4%–18.4% for MP-DOM), the component was present as a common fluorescence feature of both DOM groups, hampering the clear discrimination between the two groups. Taken together, in this study, C1 and C3 were assigned as (NOM-dominating) humic-like and (MP-dominating) protein/phenol-like components, and C2 as a typical humic-like component (Table S3).

3.2. Changes in optical indices with varying abundances of MP-DOM in the mixtures with NOM

The changes in the selected spectroscopic indices with increasing MP-DOM carbon content in the mixtures with aquatic NOM are shown in Fig. 3. Except for some indices (E2/E4, E3/E4, BIX, and FI), most measured optical indices showed significant relationships with increasing MP-DOM fraction ($p \leq 0.001$). Notably, the mixing experiments were conducted with the same DOC concentration (i.e., 1 mg-C/L), so the investigated indices should be dependent only on the physical mixing ratios of the two end-members. The observed changes in the indices with increasing MP-DOM abundance presented one of the following four patterns: (1) a linear decreasing trend, which was shown by the humic-like fluorescence-related indices (i.e., peaks H and L, HIX, C1, and C2); (2) a linear increasing trend, which was led by $S_{275–295}$, peak P, C3, and the ratio of peak H to L (H/L); (3) a nonlinear decreasing trend, which was revealed by the absorption coefficients at 254 nm and 355 nm; and (4) a nonlinear increasing trend exhibited by the $(H + P)$/L ratio (Fig. 3).

The optical indices showing decreasing trends were all related to the DOM aromatic carbon structure, which included humic-like fluorescence and HIX. In contrast, the protein-/phenol-like fluorescence properties presented an increasing trend with higher MP-DOM fractions, which was well matched with our previous observation as well as other prior reports on the release of predominant protein-like fluorophores from commercial plastics in contact with water (Lee et al., 2020a). The dominance of protein-/phenol-like fluorescence features can be attributed in part to the release of plastic additives from commercial plastics, which are often detected by fluorescence spectroscopy in the wavelength ranges related to protein- or phenol-like fluorescence (Spagnuolo et al., 2017; Suhrhoff and Scholz-Böttcher, 2016). Except for the H/L ratio, we observed a common trend, in which these spectral ratios showed better capabilities for MP-DOM detection in the mixtures than those directly obtained from a particular wavelength, as shown by their higher R^2 values (R^2 = 0.6169–0.8566 versus 0.1706–0.8213) among the regressions with p-values of ≤0.001 (Fig. 3).

3.3. Evaluation of source discrimination indices for MP-DOM

The source discrimination capability of the selected optical indices was evaluated by comparing (1) the p-values of the Student's t-test

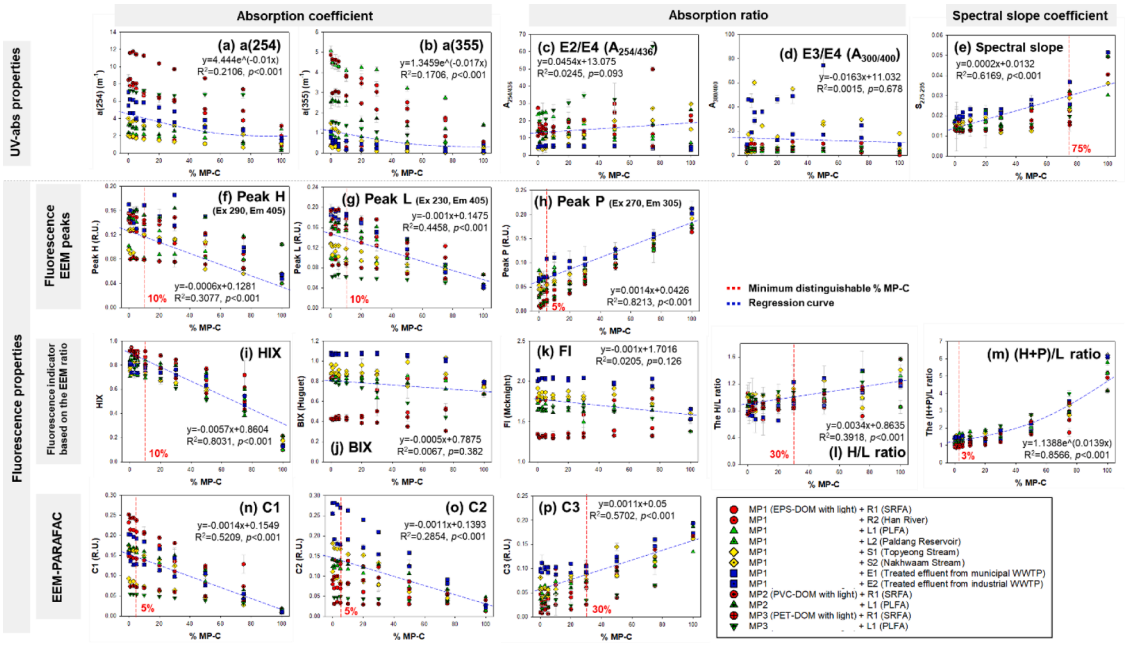

Fig. 3. Changes in selected optical indices of end-member mixtures (MP-DOM + aquatic NOM) with increasing abundance of MP-DOM. Absorption coefficients at 254 and 355 nm (a_{254} and a_{355}) (a and b, respectively). Absorption ratios at 254 to 436 nm and at 300 to 400 nm (E2/E4 and E3/E4) (c and d, respectively). Spectral slope (e). Three major EEM peaks (i.e., peaks H, L, and P) (f, g, and h). Humification index (i). Biological index (j). Fluorescence index (k). EEM peak ratios of H/L (l) and $(H + P)$/L (m). Three fluorescent components (C1 to C3) (n to p). The 0% MP-C (MP-DOM: aquatic NOM = 0:100) represents the presence of pure aquatic NOM in the mixtures, while 100% MP-C (MP-DOM: aquatic NOM = 100:0) indicates 100% MP-DOM solutions. The blue dashed lines indicate the regression curves between the optical indices and the%MP-C value. The red dashed vertical lines refer to the minimum%MP-C values resulting in p-values of <0.01 (i.e., significant difference) from the Student's *t*-test between the 0% MP-C group and the particular end-member mixtures (1, 3, 5, 10, 20, 30, 50, 75, and 100% MP-C). We interpret that lower values indicate a more sensitive index when discriminating between MP-DOM and aquatic NOM in the mixtures. The MP-DOM samples were obtained from the UV irradiation condition.

between 0%- and 100%-MP-DOM samples; (2) the R^2 values of the linear regressions between the optical indices and MP-DOM fraction, in which nonlinear relationships were log-transformed to make them comparable with linear indices; and (3) the minimum distinguishable%MP-DOM value, which was defined by the minimum%MP-DOM value with a *p*-value of <0.05, based on the Student's *t*-test with 0% MP-DOM samples (or pure aquatic NOM samples) (Lee et al., 2018; Yang and Hur, 2014) (Table 1). The first evaluation criterion refers to the minimum requirement for the source discrimination indicator between the two end-members (i.e., MP-DOM vs. aquatic NOM), while the second one can serve as a measure of the index's accuracy to estimate the relative abundance of MP-DOM in the mixture with aquatic NOM. Thus, the index revealing a statistically significant difference between two end-member groups with a relatively higher R^2 value can be regarded as a better surrogate for detecting plastic-derived DOM in environmental samples containing aquatic NOM. For example, although C2 exhibited a significant difference between the two end-member groups, it inaccurately distinguish MP-DOM from typical NOM solutions because of the relatively low R^2 value (0.2854). Among the tested optical indices, three optical indices satisfied the first two criteria: peak P, HIX, and the $(H + P)$/L ratio. Finally, the minimum distinguishable MP-DOM% was compared for the three indices, which helped to choose the best source discrimination index with a high accuracy for MP-DOM detection in environmental samples. Among the three candidates, the newly suggested EEM peak ratio, $(H + P)$/L, presented the lowest MP-DOM% (i.e., 3%), which suggests that it is the most robust and reliable indicator for discriminating plastic-derived carbon sources in aquatic systems. (Romera-Castillo et al., 2018) have demonstrated that up to 10% of DOC in sea surface microlayer could originate from wasted floating plastics in the polluted aquatic environment. Although the estimate was extrapolated from the results of laboratory experiments, the study implies that the discrimination level of our proposed index is sufficient to detect MP-DOM in any water body suffering from severe plastic pollution.

3.4. *Applicability of MP-DOM discrimination indices for environmental samples*

Although the $(H + P)$/L ratio performs the best as a source discriminator for MP-DOM among the three candidate indices, it is still necessary to further evaluate its feasibility for environmental samples containing MP particles. To this end, additional leaching tests were conducted using commercial EPS plastics (500 and 1000 EPS per liter) for 7 days under dark and UV irradiation conditions in artificial freshwater, as well as in two different NOM solutions (i.e., Paldang reservoir: L2; treated effluent: E2) (Table 2 and Fig. S7). For all the prepared solutions, significant changes in the three indices occurred as a result of the production of MP-DOM or leaching (Student's *t*-test, $p < 0.05$), which was in contrast to the insignificant difference in the DOC concentrations before versus after leaching ($p = 0.061$ for 500 pieces of EPS/L, $p = 0.052$ for 1000 pieces of EPS/L) (Table 2). The leaching-driven changes were more pronounced for the samples under UV irradiation than for those in the dark. For example, the intensity of peak P increased by 1.86- to 2.94-times in the dark-treated samples after leaching, while the increase reached 2.36- to 3.69-times in the irradiated counterparts when 1000 pieces per liter were added to the solutions. Irrespective of the added amount of plastics and the leaching conditions, the new fluorescence indicator, $(H + P)$/L, showed the most significant difference in the background solutions with and without MPs ($p < 0.01$ for all cases). These findings are noteworthy because the amount of added plastics falls within the ranges previously reported in freshwater (0.01 to 519 pieces per liter) and wastewater effluent samples (338 to 1473 pieces per liter) (Pivokonsky et al., 2018). Furthermore, the $(H + P)$/L ratio showed relatively small variations (2.0- to 5.5-fold) across the different background NOM solutions (i.e., artificial freshwater,

Table 1
Changes in the spectroscopic indices with increasing MP-DOM fraction (%MP-C) in the mixture with aquatic NOM.

Spectroscopic indices for MP-DOM discrimination			Tendency of change	Relationship type (Linear or Nonlinear)	*p*-values from Student's *t*-test between 0% and 100% MP-C groups[a]	R^2 [b]	Minimum detectable% MP-DOM[c]	Applicability for MP-DOM source discrimination
UV-visible properties	Absorption coefficient	a_{254}	↓	Nonlinear	0.0114	0.2106	–	
		a_{355}	↓	Nonlinear	0.0021	0.1706	–	
	Absorption ratio	E2/E4 ($A_{254/436}$)	n.	–	0.2015	0.0245	–	
		E3/E4 ($A_{300/400}$)	n.	–	0.4431	0.0015	–	
	Spectral slope	$S_{275–295}$	↑	Linear	<0.001	0.6169	75	√
Fluorescence properties	EEM peak intensities	Peak H (Ex 290, Em 405)	↓	Linear	<0.001	0.3077	10	√
		Peak L (Ex 230, Em 405)	↓	Linear	<0.001	0.4458	10	√
		Peak P (Ex 270, Em 305)	↑	Linear	<0.001	0.8213	5	√√√
	Fluorescence peak ratios	HIX	↓	Linear	<0.001	0.8031	10	√√√
		BIX	n.	–	0.1174	0.0067	–	
		FI	n.	–	0.0061	0.0205	–	
		H/L	↑	Linear	0.1650	0.3918	–	
		$(H + P)$/L	↑	Nonlinear	<0.001	0.8566	3	√√√
	EEM-PARAFAC	C1	↓	Linear	<0.001	0.5209	5	√
		C2	↓	Linear	<0.001	0.2854	5	√
		C3	↑	Linear	<0.001	0.5702	30	√

n. : no change in the trend (or no relationship).
[a] The *p*-values obtained from the Student's *t*-test between 0 and 100% MP-C fraction of end-member mixtures.
[b] Data from the linear regressions (nonlinear indices are log-transformed to make them comparable with linear indices).
[c] *p*-values of <0.05 obtained from paired t-tests between the 0% MP-C group and the mixture samples (1, 3, 5, 10, 20, 30, 50, 75, and 100% MP-C).
√: the p-value of the Student's *t*-test between 0 and 100% MP-C groups is less than 0.001.
√√: the p-value of the Student's *t*-test between 0 and 100% MP-C groups is less than 0.001, and the correlation of determination (R^2) is higher than 0.8.
√√√: the p-value of the Student's *t*-test between 0 and 100% MP-C groups is less than 0.001, the correlation of determination (R^2) is higher than 0.8, and the minimum distinguish%MP-C is the top three highest among the tested indices.

reservoir, and effluents) when compared with the other indices (DOC: 0.96- to 17.3-fold, HIX: 0.93- to 7.0-fold, and peak P: 1.6- to 53.5-fold). The intensity of peak P increased by 48-times in artificial freshwater containing 1000 EPS per liter under UV-irradiation, which changed from 0.002 ± 0.000 R.U. in the control samples (i.e., no MP) to 0.096 ± 0.001 R.U., while it increased by only six-folds in the effluent samples (i.e., E2), varying from 0.017 ± 0.001 R.U. to 0.104 ± 0.006 R.U. In contrast, the $(H + P)$/L ratio showed relatively stable incremental changes against the three NOM background solutions, showing 5.0- to 5.5-fold changes across the three NOM solutions containing 1000 pieces of EPS per liter compared to the control samples in the light condition. The results suggest that the new index is not significantly affected by the sources of NOM as the background; therefore, it can be effectively used to track MP-DOM in environmental samples. The incorporation of peaks H and L in the new index seems to partially resolve the overlapping problem of peak P in MP-DOM with the protein-/phenol-like fluorescence in the NOM samples. Another benefit is that the $(H + P)$/L ratio as a source discriminator is not dependent upon the concentrations of samples. In this work, the excellent discrimination capability of the $(H + P)$/L ratio for MP-DOM and the minimal interference from NOM background solutions suggest that the ratio is a robust indicator for detecting the presence of plastic-derived DOM in MP-polluted aquatic systems that are affected by various NOM sources.

3.5. Limitations and environmental implications for future studies

Our results identified unique fluorescence features of MP-DOM that can be distinguished from aquatic NOM from various sources. Based on a careful comparison of the EEM features between MP-DOM and aquatic NOM groups, a new source discrimination indicator was proposed; we demonstrate that the new indicator, $(H + P)$/L, has higher sensitivity and accuracy in detecting MP-DOM presence in environmental samples relative to other commonly used optical descriptors for NOM, as well as to other fluorescence features uniquely observed in MP-DOM. The new index was a robust source discriminator because the value showed little variability with background NOM sources. However, a limitation of this study was that the new index was only evaluated for MP-DOM leached from a few plastic types. Furthermore, the effect of background NOM concentrations on the relationships between optical indices and MP-DOM abundance was not fully considered in the end-member mixing analysis. Therefore, further comparative experiments are required to confirm whether the new index is applicable to other plastic materials and/or other background NOM solutions with varying DOC concentrations. In the same vein, complementary studies need to be conducted to extend its applicability to a wider range of environmental samples including those presenting an extremely high peak P (e.g., petroleum industry wastewater), which might lower the discrimination capability of the $(H + P)$/L ratio.

Tracking the potential alternation in the suggested index during natural transformation processes of DOM, such as microbial-/photo-degradation or interactions with other media, is another interesting topic for future investigations, which can help strengthen the feasibility of source discrimination in the field. In particular, considering the dominant presence of protein/phenol-like fluorescence in MP-DOM and the strong association between the peak intensity and the liability of DOM, which is well documented in the literature, the effect of biodegradation on the change in the new index, $(H + P)$/L, should be further explored in the future. Various leaching conditions using different pH, ionic strengths, and sizes of plastic pieces should also be tested to enhance the robustness of the new source discriminator. Finally,

Table 2
Comparison of DOC concentrations and three pre-selected source discrimination indices for MP-DOM in the MP-containing NOM solutions.

MP concentrations	Control (No MP)				500 EPS-pieces/L				1000 EPS-pieces/L			
Background solution	(Artificial freshwater)		(Lake-L2)		(Artificial freshwater)		(Lake-L2)		(Artificial freshwater)		(Lake-L2)	
Leaching condition	(Dark)	(Light)	(Dark)	(Light)	(Dark)	(Light)	(Dark)	(Light)	(Dark)	(Light)	(Dark)	(Light)
DOC (mg-C/L)	0.08 ±0.01	0.04 ±0.00	0.97 ±0.08	0.41 ±0.02	0.10 ±0.03	0.46 ±0.01	0.93 ±0.02	1.56 ±0.02	0.12 ±0.04	0.69 ±0.01	0.98 ±0.07	1.57 ±0.01
					$p = 0.061$				$p = 0.052$			
HIX	0.45 ±0.04	0.28 ±0.02	0.71 ±0.03	0.61 ±0.07	0.15 ±0.05	0.06 ±0.02	0.76 ±0.01	0.32 ±0.02	0.12 ±0.06	0.04 ±0.01	0.75 ±0.02	0.31 ±0.05
					$p = 0.025$				$p = 0.017$			
Peak P (R.U.)	0.003 ±0.001	0.002 ±0.000	0.005 ±0.003	0.002 ±0.000	0.018 ±0.009	0.053 ±0.001	0.024 ±0.002	0.069 ±0.003	0.034 ±0.014	0.096 ±0.001	0.029 ±0.006	0.107 ±0.015
					$p = 0.012$				$p = 0.013$			
$(H + P)$/L ratio	1.55 ±0.25	1.11 ±0.02	1.05 ±0.11	1.04 ±0.04	3.17 ±0.96	4.45 ±0.10	2.08 ±0.02	4.32 ±0.06	4.14 ±0.55	5.99 ±0.11	2.70 ±0.07	5.19 ±0.03
					***p<0.01**				***p<0.01**			

MP concentrations	Treated effluent-E2)				Treated effluent-E2)			
Background solution								
Leaching condition	(Dark)	(Light)	(Dark)	(Light)	(Dark)	(Light)	(Dark)	(Light)
DOC (mg-C/L)	0.93 ±0.03	0.35 ±0.01	1.32 ±0.00	1.46 ±0.01	1.35 ±0.03	1.55 ±0.01		
HIX	0.82 ±0.02	0.60 ±0.03	0.54 ±0.01	0.53 ±0.05	0.56 ±0.01	0.49 ±0.02		
Peak P (R.U.)	0.023 ±0.002	0.017 ±0.001	0.036 ±0.007	0.067 ±0.004	0.044 ±0.001	0.104 ±0.006		
$(H + P)$/L ratio	1.08 ±0.03	0.98 ±0.02	2.56 ±0.13	4.11 ±0.19	2.91 ±0.13	5.45 ±0.25		

* p-values of <0.001 obtained from paired t-tests between control group and the MP-containing NOM samples (500 and 1000 EPS-pieces/L).

encouraged by the finding that the distinctive fluorescence signal of plastic-derived DOM is enhanced by UV irradiation on MPs, future studies should focus on optimizing conditions to produce a closed detection system equipped with an artificial UV irradiation to maximize the plastic-related signal in environmental samples. The system could be further developed into a cost-effective and fast screening tool to complement the conventional time-consuming detection methods for MP contamination, such as particle counting, FT-IR, and mass spectroscopy.

4. Conclusions

Given that plastic waste is a global fast-growing environmental issue and non-negligible amount of DOM could be leached from the plastic in aquatic environment, the quantitative tracking of MP-DOM in the presence of aquatic NOM is important for fully understand the fate and the dynamics of DOM in aquatic systems suffering from plastic pollution. This study took advantage of the unique spectroscopic properties of plastic-derived DOM generated under dark and UV irradiation conditions to propose an optical source discrimination index for the presence of MP-DOM in environmental samples. Two distinct changing patterns were identified for the tested optical indices during the mixing of two contrasting DOM end-members (i.e., MP-DOM and typical aquatic NOM samples). After careful examination, a new optical descriptor, the ratio of $(H + P)$/L, was proposed to track the plastic-originated carbon in the presence of NOM solutions. Based on the results, the following key conclusions were determined:

(1) Three prominent peaks were commonly observed in the EEM spectra of MP-DOM, particularly UV-irradiated peaks, which included one phenol-/protein-like fluorescence (peak P) and two humic-like fluorescence peaks (peaks H and L). Distinctive features between MP-DOM and aquatic NOM led to the establishment of a source discrimination index consisting of the three peaks, which was defined as '$(H + P)$/L'.
(2) The source-tracking index showed a clear change during end-member mixing. Compared with other well-known optical indices, the ratio of $(H + P)$/L served as a good surrogate for discriminating the MP-C source fraction, which was corroborated by the highest positive correlation and the minimum detectable% MP-C ($R^2 = 0.8767$, 3% of MP fraction) among the tested indices for two MP-DOM and eight aquatic NOM solutions.
(3) Irrespective of the added amount of MPs and the leaching conditions, the new fluorescence index presented the highest distinction between NOM solutions with and without the plastic. The index was relatively invariable between the sources of NOM background solutions, suggesting that the $(H + P)$/L ratio can serve as a robust indicator of plastic-derived DOM in the presence of aquatic NOM.

Declaration of Competing Interest

The authors declare that they have no known competing financial interests or personal relationships that could have appeared to influence the work reported in this paper.

Acknowledgments

This work was supported by grants from the National Research Foundation of Korea (NRF), funded by the Korean government (2020R1A2C2007248, 2020R1A4A2002823).

Supplementary materials

Supplementary material associated with this article can be found, in the online version, at doi:10.1016/j.watres.2021.117833.

References

Alimi, O.S., Farner Budarz, J., Hernandez, L.M., Tufenkji, N., 2018. Microplastics and nanoplastics in aquatic environments: aggregation, deposition, and enhanced contaminant transport. Environ. Sci. Technol. 52 (4), 1704–1724.

Battin, T.J., 1998. Dissolved organic matter and its optical properties in a blackwater tributary of the upper Orinoco river, Venezuela. Org. Geochem. 28 (9–10), 561–569.

Carstea, E.M., Bridgeman, J., Baker, A., Reynolds, D.M., 2016. Fluorescence spectroscopy for wastewater monitoring: a review. Water Res. 95, 205–219.

Chae, Y., An, Y.-.J., 2018. Current research trends on plastic pollution and ecological impacts on the soil ecosystem: a review. Environ. Pollut. 240, 387–395.

Claret, F., Schäfer, T., Bauer, A., Buckau, G., 2003. Generation of humic and fulvic acid from Callovo-Oxfordian clay under high alkaline conditions. Sci. Total Environ. 317 (1–3), 189–200.

Coble, P.G., 1996. Characterization of marine and terrestrial DOM in seawater using excitation-emission matrix spectroscopy. Mar. Chem. 51 (4), 325–346.

Derrien, M., Shin, K.-.H., Hur, J., 2019. Assessment on applicability of common source tracking tools for particulate organic matter in controlled end member mixing experiments. Sci. Total Environ. 666, 187–196.

Derrien, M., Yang, L., Hur, J., 2017. Lipid biomarkers and spectroscopic indices for identifying organic matter sources in aquatic environments: a review. Water Res. 112, 58–71.

Egessa, R., Nankabirwa, A., Ocaya, H., Pabire, W.G., 2020. Microplastic pollution in surface water of Lake Victoria. Sci. Total Environ. 741, 140201.

Galgani, L., Engel, A., Rossi, C., Donati, A., Loiselle, S.A., 2018. Polystyrene microplastics increase microbial release of marine Chromophoric Dissolved Organic Matter in microcosm experiments. Sci. Rep. 8 (1), 14635.

Galloway, T.S., Cole, M., Lewis, C., 2017. Interactions of microplastic debris throughout the marine ecosystem. Nat. Ecol. Evol. 1 (5), 1–8.

Gewert, B., Plassmann, M., Sandblom, O., MacLeod, M., 2018. Identification of chain scission products released to water by plastic exposed to ultraviolet light. Environ. Sci. Technol. Lett. 5 (5), 272–276.

He, W., Lee, J.-.H., Hur, J., 2016. Anthropogenic signature of sediment organic matter probed by UV–Visible and fluorescence spectroscopy and the association with heavy metal enrichment. Chemosphere 150, 184–193.

Helms, J.R., Stubbins, A., Ritchie, J.D., Minor, E.C., Kieber, D.J., Mopper, K., 2008. Absorption spectral slopes and slope ratios as indicators of molecular weight, source, and photobleaching of chromophoric dissolved organic matter. Limnol. Oceanogr. 53 (3), 955–969.

Heo, J., Yoon, Y., Kim, D.-H., Lee, H., Lee, D., Her, N., 2016. A new fluorescence index with a fluorescence excitation-emission matrix for dissolved organic matter (DOM) characterization. Desalination Water Treat. 57 (43), 20270–20282.

Hu, C., Muller-Karger, F.E., Zepp, R.G., 2002. Absorbance, absorption coefficient, and apparent quantum yield: a comment on common ambiguity in the use of these optical concepts. Limnol. Oceanogr. 47 (4), 1261–1267.

Huang, Y., Wong, C., Zheng, J., Bouwman, H., Barra, R., Wahlström, B., Neretin, L., Wong, M.H., 2012. Bisphenol A (BPA) in China: a review of sources, environmental levels, and potential human health impacts. Environ. Int. 42, 91–99.

Huguet, A., Vacher, L., Relexans, S., Saubusse, S., Froidefond, J.-M., Parlanti, E., 2009. Properties of fluorescent dissolved organic matter in the Gironde Estuary. Org. Geochem. 40 (6), 706–719.

Jaffé, R., Cawley, K.M., Yamashita, Y., 2014. Applications of excitation emission matrix fluorescence with parallel factor analysis (EEM-PARAFAC) in assessing environmental dynamics of natural dissolved organic matter (DOM) in aquatic environments: a review. Acs. Sym. Ser. 27–73.

Kim, J.-M., Park, J.-D., Noh, H.-R., Han, M.-S., 2002. Changes of seasonal and vertical water quality in Soyang and Paldang river-reservoir system, Korea. Korean J. Ecol. Envir. 35 (1), 10–20.

Kowalczuk, P., Tilstone, G.H., Zabłocka, M., Röttgers, R., Thomas, R., 2013. Composition of dissolved organic matter along an Atlantic Meridional Transect from fluorescence spectroscopy and parallel factor analysis. Mar. Chem. 157, 170–184.

Lawaetz, A.J., Stedmon, C.A., 2009. Fluorescence intensity calibration using the raman scatter peak of water. Appl. Spectrosc. 63 (8), 936–940.

Lee, M.-H., Osburn, C.L., Shin, K.-H., Hur, J., 2018. New insight into the applicability of spectroscopic indices for dissolved organic matter (DOM) source discrimination in aquatic systems affected by biogeochemical processes. Water Res. 147, 164–176.

Lee, Y.K., Hong, S., Hur, J., 2021. Copper-binding properties of microplastic-derived dissolved organic matter revealed by fluorescence spectroscopy and two-dimensional correlation spectroscopy. Water Res. 190, 116775.

Lee, Y.K., Hur, J., 2020. Adsorption of microplastic-derived organic matter onto minerals. Water Res., 116426

Lee, Y.K., Murphy, K., Hur, J., 2020a. Fluorescence signatures of dissolved organic matter leached from microplastics: polymers and additives. Environ. Sci. Technol.

Lee, Y.K., Romera-Castillo, C., Hong, S., Hur, J., 2020b. Characteristics of microplastic polymer-derived dissolved organic matter and its potential as a disinfection byproduct precursor. Water Res., 115678

Li, P., Hur, J., 2017. Utilization of UV-Vis spectroscopy and related data analyses for dissolved organic matter (DOM) studies: a review. Crit. Rev. Env. Sci. Tec. 47 (3), 131–154.

Li, P., Lee, S.H., Lee, S.H., Lee, J.-.B., Lee, Y.K., Shin, H.-S., Hur, J., 2016. Seasonal and storm-driven changes in chemical composition of dissolved organic matter: a case study of a reservoir and its forested tributaries. Environ. Sci. Pollut. Res. 23 (24), 24834–24845.

Luo, H., Xiang, Y., He, D., Li, Y., Zhao, Y., Wang, S., Pan, X., 2019. Leaching behavior of fluorescent additives from microplastics and the toxicity of leachate to Chlorella vulgaris. Sci. Total Environ. 678, 1–9.

Majedi, S.M., Kelly, B.C., Lee, H.K., 2014. Combined effects of water temperature and chemistry on the environmental fate and behavior of nanosized zinc oxide. Sci. Total Environ. 496, 585–593.

McKnight, D.M., Boyer, E.W., Westerhoff, P.K., Doran, P.T., Kulbe, T., Andersen, D.T., 2001. Spectrofluorometric characterization of dissolved organic matter for indication of precursor organic material and aromaticity. Limnol. Oceanogr. 46 (1), 38–48.

Navalon, S., Alvaro, M., Garcia, H., 2011. Analysis of organic compounds in an urban wastewater treatment plant effluent. Environ. Technol. 32 (3), 295–306.

Ohno, T., 2002. Fluorescence inner-filtering correction for determining the humification index of dissolved organic matter. Environ. Sci. Technol. 36 (4), 742–746.

Phong, D.D., Hur, J., 2015. Insight into photocatalytic degradation of dissolved organic matter in UVA/TiO2 systems revealed by fluorescence EEM-PARAFAC. Water Res. 87, 119–126.

Pivokonsky, M., Cermakova, L., Novotna, K., Peer, P., Cajthaml, T., Janda, V., 2018. Occurrence of microplastics in raw and treated drinking water. Sci. Total Environ. 643, 1644–1651.

Potthoff, A., Oelschlägel, K., Schmitt-Jansen, M., Rummel, C.D., Kühnel, D, 2017. From the sea to the laboratory: characterization of microplastic as prerequisite for the assessment of ecotoxicological impact. Integr. Environ. Assess. 13 (3), 500–504.

Romera-Castillo, C., Pinto, M., Langer, T.M., Álvarez-Salgado, X.A., Herndl, G.J., 2018. Dissolved organic carbon leaching from plastics stimulates microbial activity in the ocean. Nat. Commun. 9 (1), 1430.

Shen, M., Song, B., Zhu, Y., Zeng, G., Zhang, Y., Yang, Y., Wen, X., Chen, M., Yi, H., 2020. Removal of microplastics via drinking water treatment: current knowledge and future directions. Chemosphere 251, 126612.

Shi, Y., Liu, P., Wu, X., Shi, H., Huang, H., Wang, H., Gao, S., 2021. Insight into chain scission and release profiles from photodegradation of polycarbonate microplastics. Water Res. 195, 116980.

Spagnuolo, M., Marini, F., Sarabia, L., Ortiz, M., 2017. Migration test of Bisphenol A from polycarbonate cups using excitation-emission fluorescence data with parallel factor analysis. Talanta 167, 367–378.

Su, L., Sharp, S.M., Pettigrove, V.J., Craig, N.J., Nan, B., Du, F., Shi, H., 2020. Superimposed microplastic pollution in a coastal metropolis. Water Res. 168, 115140.

Suhrhoff, T.J., Scholz-Böttcher, B.M., 2016. Qualitative impact of salinity, UV radiation and turbulence on leaching of organic plastic additives from four common plastics—A lab experiment. Mar. Pollut. Bull. 102 (1), 84–94.

Weishaar, J.L., Aiken, G.R., Bergamaschi, B.A., Fram, M.S., Fujii, R., Mopper, K., 2003. Evaluation of specific ultraviolet absorbance as an indicator of the chemical composition and reactivity of dissolved organic carbon. Environ. Sci. Technol. 37 (20), 4702–4708.

Yang, L., Hur, J., 2014. Critical evaluation of spectroscopic indices for organic matter source tracing via end member mixing analysis based on two contrasting sources. Water Res. 59, 80–89.

Zhu, L., Zhao, S., Bittar, T.B., Stubbins, A., Li, D, 2020. Photochemical dissolution of buoyant microplastics to dissolved organic carbon: rates and microbial impacts. J. Hazard. Mater. 383, 121065.